



The electrochemical behaviour of CuZn under conditions of illumination

Amy L. Rudd, Carmel B. Breslin *

Department of Chemistry, National University of Ireland Maynooth, Maynooth, Co. Kildare, Ireland

Received 15 December 1999; received in revised form 14 April 2000

Abstract

The influence of UV illumination on the passive behaviour of Cu₃₇Zn in pH 9.2 and 13.0 chloride-containing electrolytes was studied using potentiodynamic polarisation tests, cyclic voltammetry and complex impedance spectroscopy. It was found that UV illumination exerted a slight activating effect on the passive behaviour in the alkaline pH 13.0 solution, with slightly higher passive current densities being recorded under conditions of illumination. A more pronounced UV illumination effect was observed in the pH 9.2 solution. This was characterised by a 4-fold increase in the passive current density, a shift in the breakdown potential by 250 mV in the active direction, a decrease in the charge transfer resistance and an increase in the double layer capacitance. These results are explained in terms of the nature of the passive film on CuZn, which consists of a complex layer involving ZnO · xH₂O and Cu₂O/CuO. On illumination, photo-decomposition of the n-type ZnO phase occurs leading to a modification of the passive layer rendering it more susceptible to pitting attack in the chloride environments. © 2000 Elsevier Science Ltd. All rights reserved.

Keywords: Photo-decomposition; Illumination; CuZn; Impedance; Passive film; Pitting

1. Introduction

The electrochemical behaviour of pure copper and zinc and the formation of copper and zinc oxides, in alkaline and slightly alkaline solutions, have been studied extensively [1–5]. It is well known that passive films formed on pure copper consist generally of a duplex structure with an inner Cu₂O and an outer CuO layer, or hydrated CuO layer, with the composition of the phases being dependent on the solution composition and polarisation conditions [1–3,6,7]. Pure Cu₂O is a p-type semiconductor with a band-gap energy of 2.2 eV, while CuO also exhibits p-type conductivity [8]. It has been shown that the semiconducting properties of

the passive layers grown on copper depend critically on the manner in which the passive films are formed, with both p-type and n-type conductivity being reported [9–12]. On the other hand, it has been shown that the passive layers formed on pure zinc possess many properties similar to that of the non-stoichiometric ZnO [12,13], which is an n-type semiconductor with a large optical bandgap energy of approximately 3.2 eV [14,15].

Most of the studies conducted on the electrochemical behaviour of Cu–Zn alloys have centred on stress corrosion cracking and dezincification [16–18]. However, it has also been shown, using electrochemical and surface analytical techniques, that the passive layers formed on CuZn in neutral and alkaline solutions consist of a complex combination of ZnO · xH₂O and Cu₂O/CuO phases [19,20].

There have been reports that irradiation of the passive films formed on zinc, copper and copper–nickel

* Corresponding author. Tel.: +353-1-7083770; fax: +353-1-7083815.

E-mail address: cb.breslin@may.ie (C.B. Breslin).

alloys causes changes in the passive behaviour of the electrodes [21–29]. For example, Kruger [21] showed that illumination of a copper surface in water with white light reduced considerably the rate of formation of Cu_2O . Chagas et al. [22], on measuring the weight loss of copper in H_2SO_4 solutions, found that the weight loss of copper was higher under conditions of illumination. Bertocci [23], using impedance measurements on bulk Cu_2O , showed that the charge transfer resistance decreased considerably on illumination of the electrode. In other reports, it has been shown that illumination of Cu–Ni alloys renders the passive layers more resistant to the onset of localised attack [24,25]. In the case of pure zinc, it has been shown that illumination leads to an increase in the corrosion rate in chloride-containing solutions [26,27] and in alkaline solutions [28,29]. However, there have been no reports on the effects of irradiation on the passivity of CuZn alloys.

In this communication, the results of an investigation into the influence of UV illumination on the passive behaviour of CuZn in alkaline and slightly alkaline solutions are presented.

2. Experimental

Test specimens were prepared from Cu37Zn (total impurities < 6000 ppm). The electrodes were embedded in epoxy resins in a Teflon holder and electrical contact achieved by means of a copper wire threaded into the base of the metal sample. The exposed surfaces were polished to a 1200-grit finish using SiC paper. They were then cleaned in distilled water and dried under a stream of air.

The electrochemical cell consisted of a three-electrode Teflon cell with a quartz window in the base to allow irradiation of the test electrodes. A saturated calomel electrode (SCE) was used as the reference electrode and high-density graphite rods were used as the auxiliary electrodes. All potentials quoted are on the SCE scale.

The electrolytes were prepared using analytical grade reagents and distilled water. Two electrolytes were used, a borate buffer, pH 9.2 electrolyte (0.001 M NaOH, 0.025 M $\text{Na}_2\text{B}_4\text{O}_7$) and a pH 13.0 electrolyte (0.1 M NaOH, 0.025 M $\text{Na}_2\text{B}_4\text{O}_7$). In the case of the chloride-containing solutions 0.025 M NaCl was added to these electrolytes.

The illumination source was a 300 W xenon arc lamp (Oriel Model 6258). The light was passed through a water cooler to remove infrared radiation. The beam was then passed through a series of filters, lens and mirrors and focused on the stage to illuminate the entire surface of exposed electrode. The intensity of the light was measured as 250 mW cm^{-2} for polychromatic irradiation (200–900 nm) using a Spectra-Physics CW

Laser Power Meter Model 407A. A maximum temperature rise of 1.9°C was recorded over an 1800-s illumination period with this polychromatic illumination procedure.

Potentiodynamic electrochemical experiments were carried out using an EG&G Potentiostat, Model 263. In potentiodynamic tests, the electrodes were polarised cathodically for 360 s to ensure any air-formed oxides were removed, and then polarised in the anodic direction at a rate of 0.5 mV s^{-1} . In cases, where a pre-formed oxide was used, the electrode was immersed in the non-chloride containing electrolyte, pre-reduced and then subjected to a potential in the passive region for a set length of time. These electrodes were then transferred to the appropriate chloride-containing solution and polarised from the corrosion potential at a scan rate of 0.5 mV s^{-1} in the anodic direction. Cyclic voltammetry measurements were performed at a scan rate of 50 mV s^{-1} . Impedance spectra were recorded at some applied potential, using an excitation voltage of 10 mV, using a Solartron 1250 FRA and 1287 potentiostat. All impedance data were fit to appropriate equivalent circuits using a complex non-linear least squares fitting routine, using both the real and imaginary components of the data.

3. Results

In Figs. 1 and 2 representative anodic polarisation plots are shown for CuZn polarised under various conditions of illumination and non-illumination in the chloride-containing pH 13.0 and 9.2 electrolytes, respectively. The data presented in Fig. 1a were obtained by polarising the electrode, following a pre-reduction step in the dark at -1.0 V , under continuous dark conditions and continuous illumination conditions in the chloride-containing pH 13.0 electrolyte. The data recorded in the dark were characterised by an anodic oxidation peak at -400 mV , which corresponded to the formation of Cu(I) oxide, and a second oxidation peak at -120 mV which was associated with the formation of the Cu(II) oxide phase. At potentials between -100 and $+600 \text{ mV}$ a pseudo passive region was observed, while at potentials greater than $+650 \text{ mV}$ complete breakdown of the passive layer occurred. Similar features, although not identical, were seen under illumination conditions. The greatest difference between the illuminated and non-illuminated experiments lies in the magnitude of the pseudo-passive current density. For example, at 0.2 V , the current density recorded in the dark was typically $200 \mu\text{A cm}^{-2}$, whereas under illumination it ranged from about 290 to $380 \mu\text{A cm}^{-2}$. However, this photo-induced increase in the current density was not observed if the electrode was first subjected to an oxide formation step in the

absence of illumination. This can be seen clearly from the data presented in Fig. 1b where anodic polarisation plots recorded under continuous dark and illumination conditions are shown for electrodes first polarised for 2 h in the chloride-free pH 13.0 solution at 0.2 V. In this case, essentially identical plots are recorded in both cases and the oxidation peaks associated with the formation of the two copper oxides are obviously absent.

In Fig. 2a and b, similar data recorded in the chloride-containing pH 9.2 solution are shown. The data presented in Fig. 2a were recorded under continuous illumination and dark conditions following a pre-reduction step in the chloride-containing pH 9.2 solution. The plot recorded in the dark was characterised by a relatively low current of about $10 \mu\text{A cm}^{-2}$ in the potential interval of -200 to 450 mV. The oxidation peaks associated with the formation of the Cu(I) and

Cu(II) oxides were not clearly visible in this case. At potentials of approximately 820 mV, breakdown of the film occurred and this was marked by a sharp increase in the anodic current. The data recorded under continuous illumination conditions are significantly different. The anodic current density is approximately a factor of four higher, being of the order of $40 \mu\text{A cm}^{-2}$ and considerably lower breakdown potentials are recorded. However, these photo-induced effects were significantly reduced if an oxide film was first formed on the electrode in the absence of chloride. Typical data, recorded under these conditions, are shown in Fig. 2b. In this case, the electrodes were first polarised in the chloride-free pH 9.2 solution at 0.3 V under dark conditions for 2 h. The electrode was then transferred to the chloride solution and polarised under continuous dark or light conditions. Here, it can be seen that the photo-induced anodic currents are smaller and that the shift in the breakdown potential on illumination is considerably smaller. Breakdown potentials recorded under dark and light conditions can be seen more clearly by the data presented in Fig. 2c. Here, cumulative probability plots of the breakdown potentials recorded under four different sets of conditions are presented. Breakdown potential data are shown for the experiments recorded under illumination conditions without a pre-oxide formation step, under illumination conditions following a pre-oxide formation step and under dark conditions without and with a pre-oxide formation step. It can be seen clearly from these data that the greatest degree of photo-induced breakdown occurs when the electrode is not subjected to a pre-passivation process. Likewise, if an oxide layer is first formed on the electrode then illumination has a much-reduced deleterious effect on the breakdown process.

In order to investigate the nature of these differing photo effects, cyclic voltammetry and photo-potential measurements were carried out in an attempt to relate the photo-effects with the nature of the passive layers formed under these solution conditions. Typical cyclic voltammograms recorded under continuous dark conditions and illumination only during the anodic scan in the chloride-free pH 13.0 electrolyte are shown in Fig. 3a. The electrodes were first reduced at -1.5 V and then polarised at a rate of 50 mV s^{-1} in the anodic direction up to a vertex potential of 0.8 V and then the scan was reversed and the electrode polarised in the cathodic direction. In all, three separate reduction peaks can be distinguished and these are labelled on the diagram as Q1, Q2 and Q3. It can be seen from this plot that the current associated with the reduction of these peaks is higher under anodic illumination conditions. The ratio of the peak current densities (averaged over five measurements) recorded under illumination conditions and dark conditions, i.e. $I_p(\text{illum})/I_p(\text{dark})$

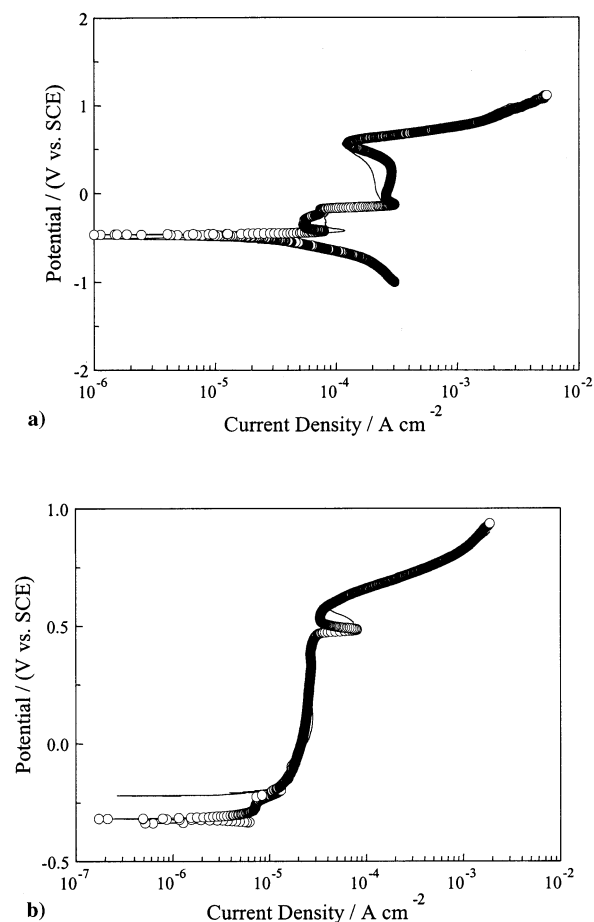


Fig. 1. (a) Anodic polarisation plots recorded in a chloride-containing pH 13.0 electrolyte under — dark and \circ illumination conditions. (b) Anodic polarisation plots recorded in a chloride-containing pH 13.0 electrolyte under — dark and \circ illumination conditions following a pre-oxide formation period of 2 h at 0.2 V in the chloride-free pH 13.0 solution.

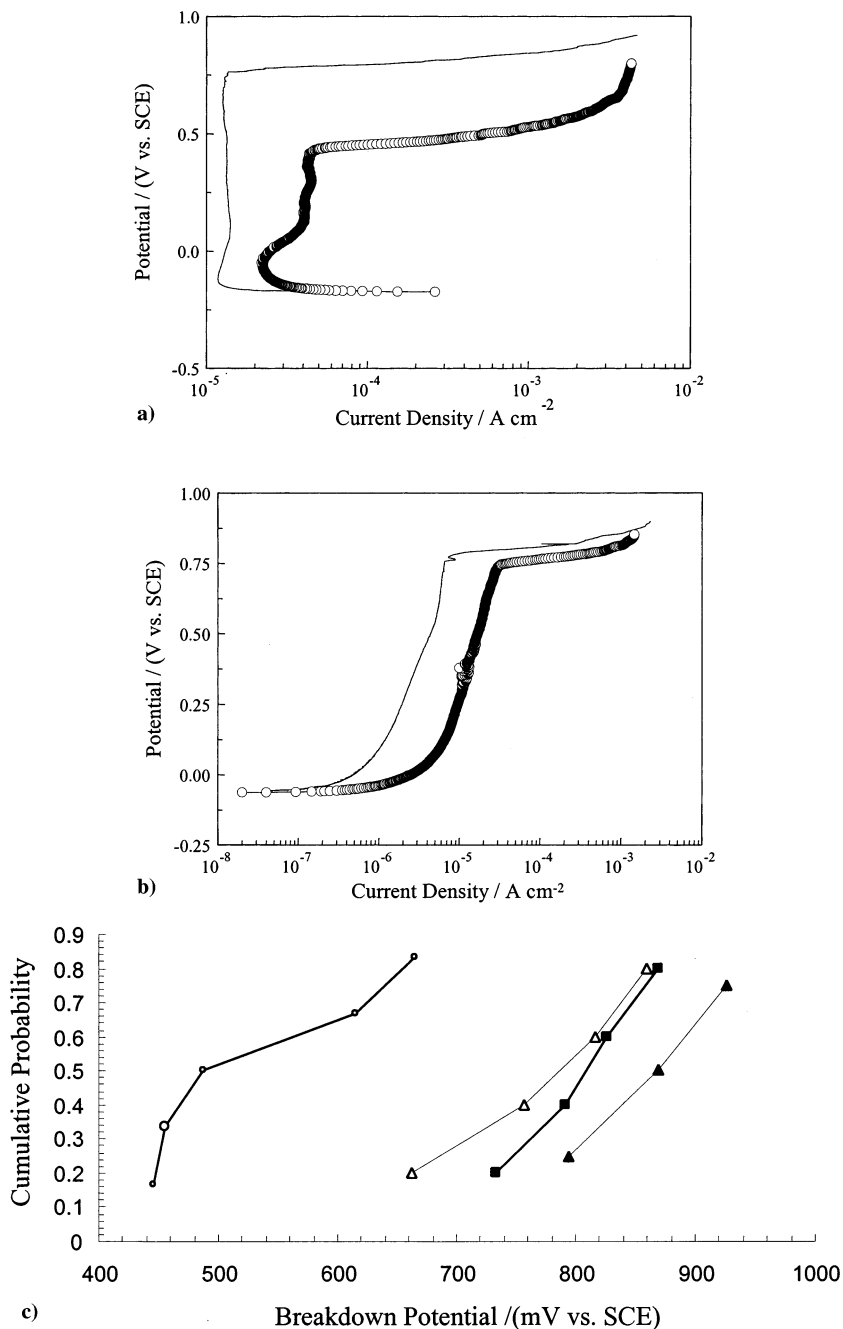
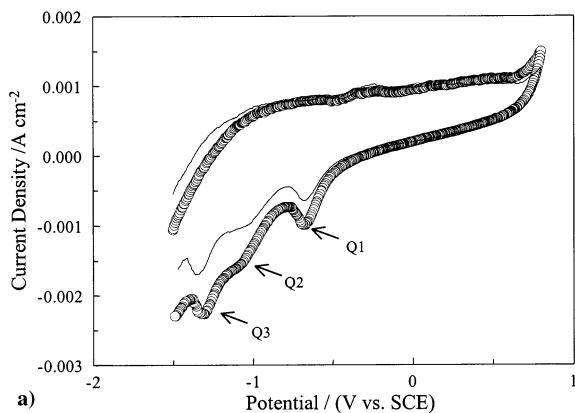


Fig. 2. (a) Anodic polarisation plots recorded in a chloride-containing pH 9.2 electrolyte under — dark and ○ illumination conditions. (b) Anodic polarisation plots recorded in a chloride-containing pH 9.2 electrolyte under — dark and ○ illumination conditions following a pre-oxide formation period of 2 h at 0.3 V in the chloride-free pH 9.2 solution. (c) Cumulative probability plots of the breakdown potentials recorded in the pH 9.2 solution under ■ dark conditions, ▲ dark conditions following pre-oxide formation, ○ light conditions, △ light conditions following pre-oxide formation.

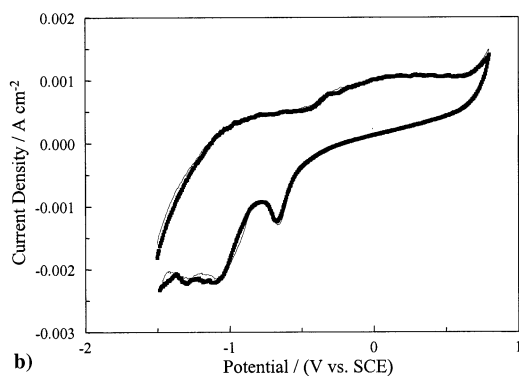
for Q1 was 1.37 ± 0.09 , while it was 1.46 ± 0.06 for Q2 and 1.38 ± 0.02 for Q3. In addition, the total reduction charge computed under dark conditions, averaged over five determinations, was 26.4 ± 1.1 mC cm⁻² compared

with 37.1 ± 2.3 mC cm⁻² under illumination conditions. This was computed over the three reduction peaks using an integration routine in which zero current was taken as the baseline.

In order to investigate whether illumination had any effect during the reductive sweep, for example a photo-facilitated reduction of the oxides, as reported in the



a)



b)

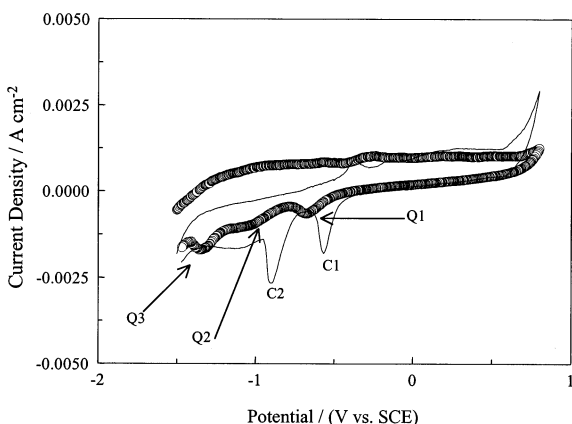


Fig. 3. (a) Cyclic voltammograms recorded in the pH 13.0 electrolyte under — continuous dark and ○ anodic illumination conditions. (b) Cyclic voltammograms recorded in the pH 13.0 electrolyte under — continuous illumination and ○ illumination only during the anodic sweep. (c) Cyclic voltammograms recorded in the pH 13.0 solution for — pure Cu and CuZn.

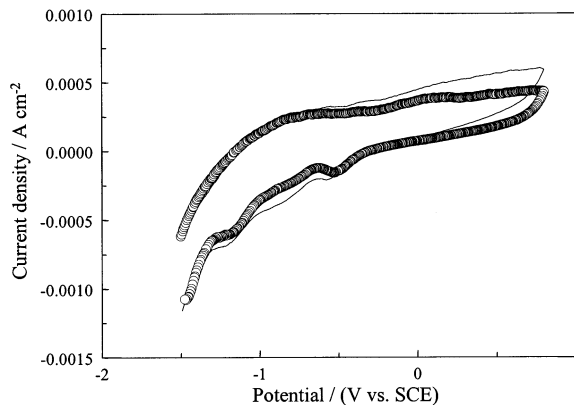


Fig. 4. Cyclic voltammograms recorded in the pH 9.2 electrolyte for CuZn under — continuous dark and ○ continuous illumination conditions.

case of pure copper [12], a second series of experiments was carried out. The results of these tests are summarised in the data presented in Fig. 3b. Here data are shown for cyclic voltammograms recorded under continuous illumination conditions and intermittent dark conditions. These intermittent dark conditions consisted of performing the anodic scans under illumination conditions and then the surface was exposed to dark conditions during the reductive sweep. As seen from these data, essentially identical profiles are obtained under continuous illumination conditions and illumination only during the oxidative sweep, which confirms that illumination does not facilitate the reduction process in this case. Indeed voltammograms identical to those presented in Fig. 3a were obtained when the light experiments consisted of exposing the electrodes to continuous illumination conditions and the dark experiments consisted of exposing the electrode to continuous dark conditions. In Fig. 3c, the cyclic voltammograms recorded for CuZn and pure Cu in the pH 13.0 electrolyte are compared. Two clear reduction peaks C1 and C2 are seen in the case of pure copper where C1 is the reduction of Cu(II) and C2 is the reduction of Cu(I). It can be seen that in the case of the CuZn system, these reduction peaks are somewhat shifted to lower potentials and are less distinct, however, it is clear that Q1 corresponds to the reduction of Cu(II), Q2 to the reduction of Cu(I) and Q3 to the reduction of Zn(II). These data are in agreement with those reported by Morales et al. [19,20], who observed a potential shift in the reduction of Cu(II) and Cu(I) for various brasses.

Typical voltammograms recorded under dark and light conditions in the chloride-free pH 9.2 solution are shown in Fig. 4. The illumination experiments were recorded under continuous illumination, but similar data were obtained if the reduction scans were recorded

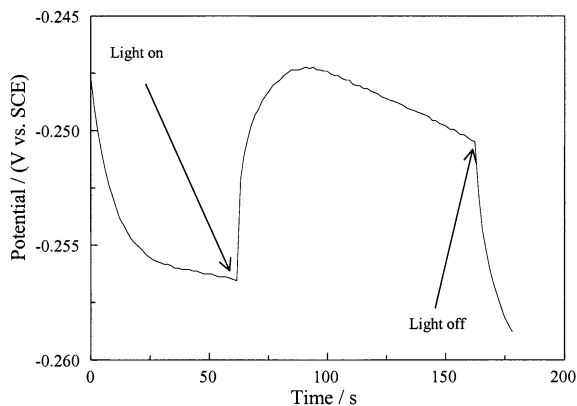


Fig. 5. Photo-potential measurement for CuZn in the pH 13.0 solution.

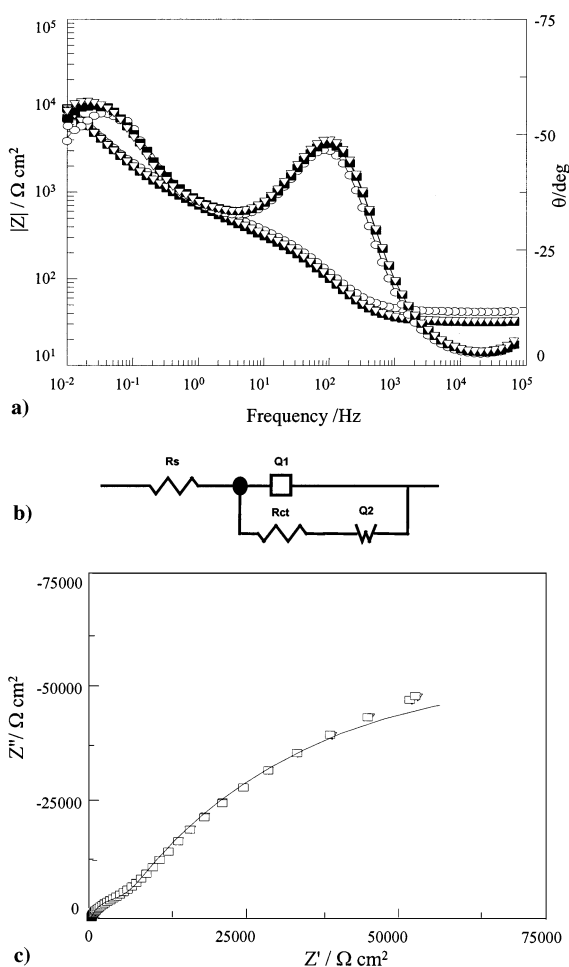


Fig. 6. (a) Impedance data recorded for CuZn polarised at 0.2 V in the pH 13.0 electrolyte under — initial dark conditions, ○ illumination conditions and ● final dark conditions. (b) Equivalent circuit used in the fitting of the impedance data. (c) Quality of fit between experimental and simulated data.

in the dark. It can be seen from a comparison of this plot with that presented in Fig. 3a that the peaks are much less defined and only the total cathodic charge could be computed. The ratio of the total cathodic charge under UV conditions and dark conditions was computed as 0.93, averaged over five determinations. Thus, under these conditions there is no evidence to suggest photo-induced growth of the passive film. However, it can be seen on comparing the data presented in Figs. 3 and 4 that significantly higher amounts of the copper and zinc oxides are formed in the more alkaline pH 13.0 solution. For example, the average peak current density, Q_2 , recorded under dark conditions was 1.50 mA cm^{-2} and $500 \mu\text{A cm}^{-2}$ in the pH 13.0 and 9.2 solutions, respectively.

A typical example of a photo-potential measurement in the pH 13.0 solution is shown in Fig. 5. The electrode was immersed in the pH 13.0 solution for 90 min and then the photo-potential was measured. The actual data shown were recorded after 90-min immersion time and were scaled to zero. The points at which the light was switched on and off were marked on the diagram. It is seen from these data that on illumination a positive photo-potential was recorded, consistent with p-type conductivity. Similar data were recorded in the pH 9.2 solution, but the magnitude of the photo-potential was somewhat lower. Typical photo-potentials were of the order of 10 and 5 mV in the pH 13.0 and 9.2 solutions, respectively. It can be inferred from these data that the complex films formed on CuZn under these conditions behave like p-type Cu(I) and Cu(II) oxides, there is no evidence of any n-type conductivity which is seen in the case of pure zinc oxide films [28].

Impedance spectra recorded under different conditions of illumination and non-illumination are shown in Figs. 6 and 7. In Fig. 6a, typical impedance plots are shown for CuZn polarised at 0.2 V under dark and illumination conditions in the pH 13.0 electrolyte. These data were recorded following an initial 150-min polarisation period at 0.2 V. The impedance data were first recorded under dark conditions, then under continuous illumination conditions followed by dark conditions. These data were fit to the equivalent circuit depicted in Fig. 6b, while the fit between the simulated and experimental data could be seen from the plot shown in Fig. 6c where simulated and experimental data were compared in a Nyquist plot. The equivalent circuit consists of R_s , which represents the solution resistance, Q_1 is the double layer capacitance, R_{CT} stands for the charge transfer resistance and Q_2 , a constant phase element with an exponent close to 0.6, which represents diffusion processes. As can be seen from the presented data, illumination has little effect on the impedance response. Indeed, the fitted parameters were essentially identical for the data collected under dark and light conditions. The charge transfer resis-

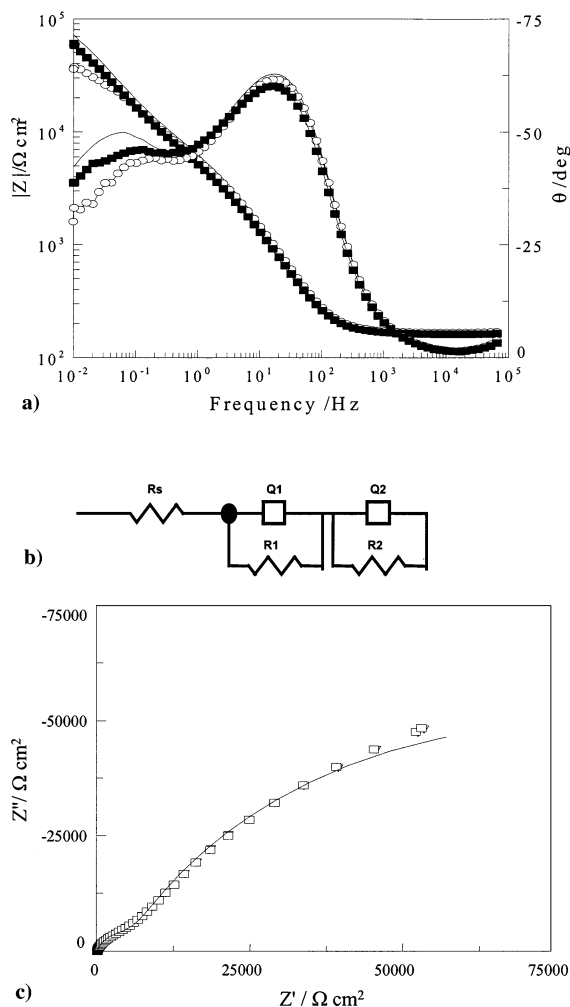


Fig. 7. (a) Impedance data recorded for CuZn polarised at 0.3 V in the pH 9.2 electrolyte under — initial dark conditions, ○ illumination conditions and ● final dark conditions. (b) Equivalent circuit used in the fitting of the impedance data. (c) Quality of fit between experimental and simulated data.

tance calculated under initial dark conditions was $400 \Omega \text{ cm}^2$, that calculated under illumination conditions was $403 \Omega \text{ cm}^2$, while that calculated under subsequent dark conditions was $381 \Omega \text{ cm}^2$. Likewise the capaci-

tance was calculated as 39, 40 and $51 \mu\text{F cm}^{-2}$ for dark, light and final dark conditions, respectively, while the diffusion term was computed as $566, 620$ and $664 \Omega^{-1} \text{ cm}^{-2} \text{ s}^n$ under dark, light and final dark conditions, respectively. Here, the greatest changes are seen following the illumination period, which suggests that the 40-min illumination period during the impedance measurements gives rise to some modification of the passive layer.

The impedance data recorded in the pH 9.2 solution are presented in Fig. 7a. Again these data were recorded following a 150-min polarisation period at 0.3 V and were recorded in the sequence dark, light and final dark conditions. The circuit used in the fitting of these data is shown in Fig. 7b, while the quality of the fit between the simulated and experimental data can be seen in Fig. 7c. A more complex circuit was required to fit these data and consists of two series R, Q couples. These data are dominated less by diffusion processes, compared with those presented in Fig. 6, and this is reflected in the exponents of the constant phase elements Q_1 and Q_2 , which are 0.90 and 0.75, respectively. The values of these fitted parameters are shown in Table 1 for dark, followed by dark, followed by light followed by final dark experiments. It can be seen from a comparison of the two initial dark experiments that the system is in a steady state and thus, the changes in the parameters are true illumination effects. These illumination effects are characterised by a decrease in R_1 and R_2 , an increase in Q_1 and an increase in Q_2 . This is consistent with a photo-induced dissolution effect. It can also be seen that the system does not revert back to its passive steady state by comparing the values of the circuit elements for the initial dark and final dark experiments. The actual significance of these circuit elements is not clear but it does seem that the R_1Q_1 couple may be related to the cupric/cuprous/zinc oxide passive layer, while the R_2Q_2 term which is more dominated by diffusion, stems from a precipitated hydroxide layer, which is dominated by zinc species. Support for this can be seen from the data presented in Fig. 8a and b. In Fig. 8a data were presented, which were recorded in the pH 9.2 solution under similar dark conditions at 0.3 V, but with pure copper. Here, two impedance measurements are shown, one recorded following a

Table 1

Circuit parameters for impedance data recorded under dark, followed by dark, followed by light and followed by dark conditions for CuZn polarised at 0.3 V in pH 9.2 solution

Condition	$R_1 (\Omega \text{ cm}^2)$	$R_2 (\Omega \text{ cm}^2)$	$Q_1 (\mu\text{F cm}^{-2})$	n_1	$Q_2 (10^{-6} \Omega^{-1} \text{ cm}^{-2} \text{ s}^n)$	n_2
Dark	4627	142.2	24.7	0.90	83.1	0.76
Dark	4636	144.3	24.8	0.90	83.5	0.76
Light	3759	53.4	26.0	0.90	94.8	0.73
Dark	3680	100.4	33.6	0.88	95.5	0.75

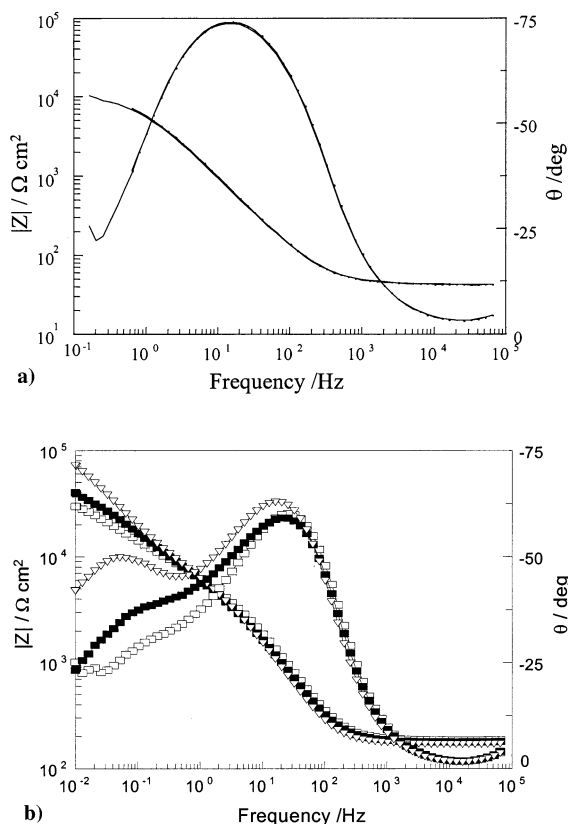


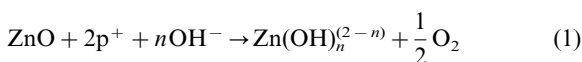
Fig. 8. (a) Impedance data recorded for pure copper polarised at 0.3 V in the pH 9.2 solution. Data recorded after — 180 min and after ... 240 min polarisation time. (b) Impedance data recorded as a function of the polarisation period for CuZn polarised at 0.3 V in the pH 9.2 solution. Data recorded after $\triangle 3.8 \times 10^3$ s, $\blacksquare 9.8 \times 10^3$ s and $\triangle 98 \times 10^3$ s.

180-min polarisation time and the second recorded following a further 60-min polarisation period. Here, the low frequency diffusion effects are not seen. Furthermore, it is seen by comparing both scans that the system remains stable and appears to be in a true steady-state condition. In Fig. 8b, impedance spectra are shown for the CuZn electrode following different polarisation periods. These data were recorded under dark conditions at an applied potential of 0.3 V in the pH 9.2 solution after different polarisation periods of 3.8×10^3 , 9.8×10^3 and 98×10^3 s. Here a clear time evolution of the data can be seen, with the low frequency diffusion region becoming more pronounced with increasing polarisation time. Thus, it seems that the low frequency diffusion region is connected with the dezincification of CuZn and the formation of precipitates of $\text{Zn}(\text{OH})_2$ at the surface/solution interface.

4. Discussion

It can be seen from these data that illumination of CuZn induces different effects depending on the solution composition, which in turn controls the passive layer composition. In the pH 13.0 solution, illumination leads to only slight changes in the polarisation characteristics and in the impedance spectra. However, in the pH 9.2 solution, illumination leads to enhanced dissolution. This can be seen from the impedance data, where the charge transfer resistance is lowered on illumination of the surface. However, the greatest effect is seen in the breakdown potentials, where illumination shifts the breakdown potential by 250 mV in the more active direction. It should be noted that these effects are not seen on polarising pure Cu under similar illumination conditions, but that the photo-decomposition of the passive layers on pure Zn is observed [28,29]. This tends to suggest that these effects are associated with the ZnO phase, and more precisely with the composition of the oxide layers formed on CuZn under these solution conditions.

Morales et al. [19,20] have shown, using XPS, that the passive layer formed on various brasses in a pH 9 borate solution consists of a complex $\text{ZnO} \cdot x\text{H}_2\text{O}/\text{Cu}_2\text{O}-\text{CuO}$ layer. The ZnO electro-formation results in a dezincification process so that a thin copper-rich layer resides at the metal/oxide interface. Indeed, it could be deduced from the photo-potential data presented in Fig. 5, which were obtained following a 90-min immersion period, that the oxide layers existing under open-circuit conditions contain a relatively large amount of copper oxides. However, the outer layers will contain ZnO as shown by Morales et al. [19,20] and the concentration of ZnO will be higher during the early stages of immersion. It is well known that ZnO is an n-type semiconductor [12–15]. On illumination with sufficiently energetic photons, electrons are promoted from the valence to the conduction band. The generated holes react with the stoichiometric ZnO to cause photo-decomposition of the ZnO lattice. This sequence of events has also been shown to occur in the case of the passive films grown on zinc in alkaline solutions, in the pH region 13–9, where photo-decomposition of the oxide layers occurs [28,29]. Since the outer regions of the passive layer on CuZn contain ZnO, then it is likely that UV illumination of this layer will lead to the photo-decomposition of the ZnO component through the reaction.



The nature of the soluble $\text{Zn}(\text{OH})_n^{(2-n)}$ species will depend on the pH of the solution, but in these alkaline conditions, the products are likely to be $\text{Zn}(\text{OH})_4^{2-}$ or $\text{Zn}(\text{OH})_3^-$. The above dissolution reaction is consis-

tent with the increase in the passive current density (Fig. 1), and the increase in the capacitance and the lower charge transfer resistance values computed under illumination conditions. The lower breakdown potentials recorded under illumination conditions may be connected with an increase in the defect nature and porosity of the passive layer, brought about by the selective decomposition of ZnO. However, this increase in the pitting susceptibility may also be connected to modifications of the protective CuO/Cu₂O oxide layers. The electrons generated from the electron-hole pair during illumination of the ZnO phase may reduce the copper oxide phase converting the CuO oxide to Cu₂O or the Cu₂O oxide to Cu.

This photoactivation effect is seen to diminish if passive layers are first formed on the electrodes by polarisation at 0.3 V for extended periods (Fig. 2b). Polarisation at this potential should favour the formation of Cu(I) and Cu(II) oxides and furthermore increase the rate of dezincification leading to a greater copper-rich passive layer. Indeed the evolution of the passive layer with time can be seen from the impedance data presented in Fig. 8b. Here, the low frequency impedance is seen to increase with polarisation time, which is consistent with a dezincification process and the precipitation of hydroxide species at the oxide/solution interface. Thus, the photo-activation effect is diminished after prolonged polarisation under these potential conditions because of a decrease in the concentration of the ZnO semiconductor phase.

The lack of any substantial photo-effect in the pH 13.0 solution seems to be connected also with the concentration of the ZnO phase in the complex passive layer. It can be seen clearly by comparing the cyclic voltammetry data in Figs. 3 and 4 that the rate of Cu(I) and Cu(II) oxide formation is considerably higher in the pH 13.0 solution. Also under these highly alkaline pH conditions ZnO is not predicted to be the stable phase [4]. Both of these effects mean that the concentration of ZnO in the complex passive layer is reduced and thus illumination has only a slight activating effect on the complex passive layer.

5. Conclusions

A significant decrease in the breakdown potential, an increase in the passive current density and lower charge transfer resistance values were observed on illumination of CuZn in pH 9.2 solutions. However, these effects were diminished, if the electrode was first subjected to an oxide formation step at 0.3 V, before the illumination experiments. A much lower photo-activation effect was observed in the pH 13.0 solution. These findings may be explained in terms of the photo-decomposition of ZnO, which exists in the complex passive layers formed on CuZn.

Acknowledgements

The authors gratefully acknowledge the support of this work by Enterprise Ireland, under the Basic Science Research Grants Award, Project Code SC/96/456.

References

- [1] B. Miller, *J. Electrochem. Soc.* 116 (1969) 1675.
- [2] L.M. Abrantes, L.M. Castillo, C. Norman, L.M. Peter, *J. Electroanal. Chem.* 163 (1984) 209.
- [3] C.H. Pyun, S.M. Park, *J. Electrochem. Soc.* 133 (1986) 2040.
- [4] D.D. Macdonald, K.M. Ismail, E. Sikora, *J. Electrochem. Soc.* 145 (1998) 3141.
- [5] T.E. Graedel, *J. Electrochem. Soc.* 136 (1989) 193.
- [6] T.D. Burleigh, *Corrosion* 45 (1989) 464.
- [7] F. Ammeloot, C. Fiaud, E.M.M. Sutter, *Electrochim. Acta* 44 (1999) 2549.
- [8] H.R. Schöppel, H. Gerischer, *Ber. Bunsenges Phys. Chem.* 77 (1973) 310.
- [9] F. Di Quarto, S. Piazza, C. Sunseri, *Electrochim. Acta* 30 (1985) 315.
- [10] E.M.M. Sutter, B. Millet, C. Fiaud, D. Lincot, *J. Electroanal. Chem.* 386 (1995) 101.
- [11] E.M.M. Sutter, C. Fiaud, D. Lincot, *Electrochim. Acta* 38 (1993) 1471.
- [12] J. Buchholz, *Surf. Sci.* 101 (1980) 146.
- [13] P. Scholl, X. Shan, D. Bonham, G.A. Prentice, *J. Electrochem. Soc.* 138 (1991) 895.
- [14] G. Heiland, E. Mollwo, F. Stockmann, *Solid State Phys.* 8 (1959) 191.
- [15] A.K. Vigh, *Electrochemistry of Metals and Semiconductors*, Marcel Dekker, New York, 1973.
- [16] H.W. Pickering, C. Wagner, *J. Electrochem. Soc.* 224 (1967) 698.
- [17] R.C. Newman, T. Shahrabi, K. Sieradzki, *Corros. Sci.* 28 (1988) 873.
- [18] J.C. Scully, *Met. Sci.* 12 (1978) 290.
- [19] J. Morales, G.T. Fernandez, S. Gonzalez, P. Esparza, R.C. Salvarezza, A.J. Arvia, *Corros. Sci.* 40 (1998) 177.
- [20] J. Morales, P. Esparza, G.T. Fernandez, G. Gonzalez, J.E. Garcia, J. Caceres, R.C. Salvarezza, A.J. Arvia, *Corros. Sci.* 37 (1995) 231.
- [21] J. Kruger, *J. Electrochem. Soc.* 106 (1959) 847.
- [22] L.V. Das Chagas, E.W. Grabner, R.S. Gonçalves, *Electrochim. Acta* 40 (1995) 1735.
- [23] U. Bertocci, *J. Electrochem. Soc.* 125 (1978) 1598.
- [24] C.B. Breslin, D.D. Macdonald, *Electrochim. Acta* 44 (1998) 643.
- [25] D.D. Macdonald, H. Brookes, M. Urquidi-Macdonald, M. Vazquez, *Corrosion* 55 (1999) 343.
- [26] E. Juzeliunas, P. Kalinauskas, A. Stankeviciute, A. Sudavicius, A. Survila, *Corrosion* 51 (1995) 673.
- [27] P. Spathis, I. Poullos, *Corros. Sci.* 37 (1995) 673.
- [28] A.L. Rudd, C.B. Breslin, *Electrochim. Acta* 45 (2000) 1571.
- [29] A.L. Rudd, C.B. Breslin, *J. Electrochem. Soc.*, 147 (2000) 1401.